Experimental determination of the shear strength of peat from standard undrained triaxial tests

Correcting for the effects of end restraint

Muraro, Stefano; Jommi, Cristina

DOI
10.1680/jgeot.18.P.346

Publication date
2021

Document Version
Accepted author manuscript

Published in
Geotechnique

Citation (APA)
Muraro, S., & Jommi, C. (2021). Experimental determination of the shear strength of peat from standard undrained triaxial tests: Correcting for the effects of end restraint. *Geotechnique*, *71*(1), 76-87. https://doi.org/10.1680/jgeot.18.P.346

Title: Experimental determination of the shear strength of peat from standard undrained triaxial tests: correcting for the effects of end restraint

Authors

Stefano Muraro *

Cristina Jommi *,**

Affiliation

* Department of Geoscience and Engineering, Delft University of Technology, Delft, the Netherlands

**Department of Civil and Environmental Engineering, Politecnico di Milano, piazza Leonardo da Vinci 32, 20133, Milano, Italy

Correspondence to

Stefano Muraro, Department of Geoscience and Engineering

Delft University of Technology, Stevinweg 1 / PO-box 5048, 2628 CN Delft / 2600 GA Delft, The Netherlands

Tel. +31 15 27 83327;

e-mail: S.Muraro@tudelft.nl

ABSTRACT

Conventional triaxial tests on peats are strongly criticised due to the very high shear strength parameters obtained from standard data elaboration, leading to unrealistic factors of safety when used in geotechnical design and assessment. Various operational approaches have been proposed in the literature to overcome this difficulty, however, they seem to lack consistent mechanical background. Part of the issues related to the shear strength evaluation of peats from triaxial tests comes from the non-uniform stress and strain states developing in the samples well before failure is attained, due to end restraint effects. Undrained triaxial compression tests were performed on reconstituted peat to examine the influence of end restraint on the deviatoric stress, excess pore pressure and deviatoric strain response. Samples were tested with standard rough end platens and with modified platens to reduce the friction between the sample and bottom and top caps. Four different initial height to diameter ratios were examined, to reduce the consequences of rough end platens on the sample response. The results indicate that end restraint contributes dramatically to overestimating the shear strength of peat, due to the increase in both the calculated deviatoric stress and the measured excess pore pressure at the bottom of the sample. Suggestions are given to quantify the influence of end restraint in the interpretation of standard data, in an attempt to suggest viable procedures to determine more reliable effective and undrained shear strength parameters form standard triaxial tests.

Keywords: Triaxial tests, Organic soils, Pore pressure, Shear strength

INTRODUCTION

In the engineering practice, the determination of shear strength of peats is a matter of debate due to the exceptionally high shear strength parameters derived from conventional laboratory tests, which lead to unrealistic factors of safety when used in geotechnical design and assessment. Direct shear and ring shear tests are sometimes adopted, although stress non-uniformity, which is amplified by the presence of fibres and by the large strains attained by peat samples, makes the results rather arguable (e.g. Landva & La Rochelle, 1983; Stark & Vettel, 1992; Farrell & Hebib, 1998; Ogino et al., 2002; Komatsu et al., 2011). In the recent practice, direct simple shear is widely preferred, assuming that more uniform stress and strain states are guaranteed compared to the direct and ring shear, that the effects of fibres stretch are prevented and, especially, that the test better replicates the deformation mode characterising failure in the field (Farrell et al., 1999; Boylan & Long, 2008; Zwanenburg et al., 2012; Den Haan & Grognet, 2014; O'Kelly, 2017). In reality, all these assumptions are debatable. Besides the stress and strain non-uniformity discussed by Wood et al. (1979), Budhu (1984) and Airey (1984) among others, recent works give clear evidence of fibres stretch in simple shear (e.g. Den Haan & Grognet, 2014), and failure mechanisms in the field dominated by lateral bulging and vertical compression, which is better mimicked in triaxial compression tests (Landva & La Rochelle, 1983; Tashiro et al., 2015).

The presence of multiple networks of fibres in natural peats is claimed to be mostly responsible for the very high shear strength parameters derived from triaxial tests, due to the strong confinement offered by the fibres stretch upon axial compression. Still at high strain levels, above 20% axial strain, the stress-strain response of fibrous peat is dominated by strain hardening behaviour, with deviatoric stress increasing almost linearly with deviatoric strain. Friction angles in the range 50° - 70° are often reported when the maximum stress ratio attained during the test is used to identify failure (Adams, 1961; Oikawa & Miyakawa, 1980; Landva & La Rochelle, 1983; Yamaguchi et al., 1985; Edil & Wang, 2000; Cola & Cortellazzo, 2005; Cheng et al., 2007). In addition, fibrous peat samples in undrained triaxial tests develop high excess pore water pressure, which can lead to null effective radial stress. The stress state can approach the tension cut off line, or even overpass it, before a failure mode can be clearly identified, which makes the choice for a representative value

for undrained shear strength extremely difficult (Kanmuri et al., 1998; Boulanger et al., 1998; Cola & Cortellazzo, 2005; Hendry et al., 2012). Different alternative operational criteria have been proposed in the literature to reduce these exceptionally high shear strength parameters, by limiting the reference deviatoric stress at failure. Some criteria are based on different extrapolation of the experimental data in the stress-strain or in the stress path planes (O'Kelly, 2017). Kanmuri et al. (1998), and more recently Hendry et al. (2012), proposed to associate failure to the start of the ultimate linear strain hardening response in undrained triaxial compression tests. Oikawa & Miyakawa (1980) suggested to identify failure as the transition between contractive and dilatant response. Alternatively, adopting strain based approaches, the mobilised shear strength at convenient axial strain thresholds has been used to define operational shear strength parameters (15% in Ogino et al. (2002) and Hayashi et al. (2012), 2% and 5% in Den Haan & Feddema (2013) from undrained compression tests, and 20% in Zhang & O'Kelly (2014) from drained compression tests). Despite these approaches being useful in the practice, they reveal absence of consistency in the strength evaluation of peats from triaxial tests.

Actually, part of this lack in consistency comes from the assumption of uniform stress and strain states of peat samples tested in triaxial compression, in spite of the extensive experimental effort in the 1960's addressing samples non-uniformities in standard triaxial devices (Shockley & Ahlvin, 1960; Rowe & Barden, 1964; Olson & Campbell, 1964; Bishop & Green, 1965; Barden & McDermott, 1965; Duncan & Dunlop, 1968). Among other factors related to the test protocol, end-restraint was recognised to affect the test interpretation, depending on the soil type and the soil sample geometry, and to justify a fictitious increase in the shear strength parameters determined from standard elaboration of triaxial test data. Few indications on end restraint effects on the response of peat samples are reported by Stark & Vettel (1992) for ring shear apparatus and by Yamaguchi et al. (1987) for direct simple shear. However, the relevance of end restraint effects on peats tested in triaxial devices does not seem to have been assessed yet.

The high compressibility and the fibres content of peats are likely to magnify the severity of stress and strain non-uniformity coming from end-restraint, which can largely bias the interpretation of triaxial test data (Rowe et al., 1984; Muraro & Jommi, 2019). The role of end restraint on the shear strength evaluation of

peat from undrained triaxial compression tests is systematically investigated here with a dedicated experimental study. Samples with different height to diameter ratio were tested, with both standard rough end platens and modified end platens, to reduce the boundary effects on the sample response. Care is given to clarify the difference between the sample behaviour and the true material behaviour in terms of deviatoric stress-strain response and excess pore pressure. The study wants to contribute to re-establish the potential of triaxial tests for reliable assessment of the effective and undrained shear strength of peats, by suggesting simple procedures to account for non-uniformity in elaborating experimental data.

EXPERIMENTAL PROGRAMME

Material

The peat used in this investigation was collected 1.0 to 1.5 m below the ground surface, at the Leendert de Boerspolder site in the Netherlands. To reduce bio-degradation, the material was stored in a climate controlled room at 10 ± 1°C and 90% relative humidity. Reconstituted peat samples were prepared by mixing the material with demineralised water to a slurry having a water content of 855%, corresponding to 1.4 times the liquid limit. The material was consolidated in a floating consolidometer under a total vertical stress of 10 kPa for 48 hours, before mounting it in the triaxial cell. Oven-drying procedures for soil classification were performed at a temperature of 60°C (Head, 2014). The specific gravity of the soil, Gs, was measured with a helium pycnometer (D5550-14, 2014). The organic content, OC, was assessed by ignition 500°C (D2974-14, 2014; Den Haan & Kruse, 2007). Table 1 reports the index properties of the tested samples. Fibre content determination gave an average value of 0.14 (D1997-13, 2013).

Fig. 1 displays a picture obtained from x-ray micro CT on the tested peat, after 2 days drying at a temperature of 14°C and relative humidity of 80%. Inorganic soil grains are visible with higher density (white spots) within the fibrous matrix. The fibrous structure is characterised by diffused small fibres having a maximum length of about 3 mm.

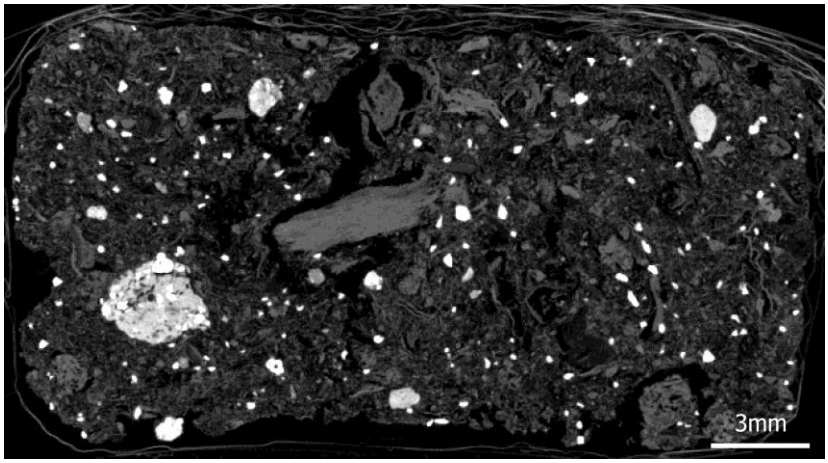

Fig. 1. Micro CT scan of the reconstituted peat used in the experimental investigation (white spots: denser inorganic constituents)

Experimental procedure

The testing programme consisted in a series of conventional undrained triaxial compression tests, and included a drained automatically adjusted K_0- compression test. The tested specimens were 38 mm in diameter and had variable height according to the prescribed initial height to diameter ratio, H_0/D_0, as reported in Table 1. The choice for testing 38 mm samples was imposed by the limited height of the triaxial apparatus for the tallest specimen. Given the maximum length of the peat fibres, the representativeness of the tested soil volume was assured (Lade, 2016). The tests were carried out using a GDS load frame triaxial apparatus with back pressure and cell pressure volume controllers and submersible 1 kN load cell, under controlled air temperature 14 ± 1°C and relative humidity 80%. The accuracy of the controllers is ± 1 kPa on pressure and ± 300 mm^3 on volume (0.15% full scale range). Thin membranes 0.25 mm thick were used. To accelerate the consolidation process, lateral filter paper was placed around the samples. To prevent "short circuit" effects between the back pressure and the pore pressure transducer located at the bottom of the sample, 10 mm of clearance were left between the lower edge of the lateral filter paper and the bottom of the samples (Head & Epps, 2014).

To reduce end restraint effects, two approaches were adopted (Fig. 2):

- increasing the height to diameter ratio for tests performed with standard rough platens;

- modifying the end platens by interposing a perforated plastic disk and a perforated nitrile membrane 0.1 mm thick between the filter paper and the sample.

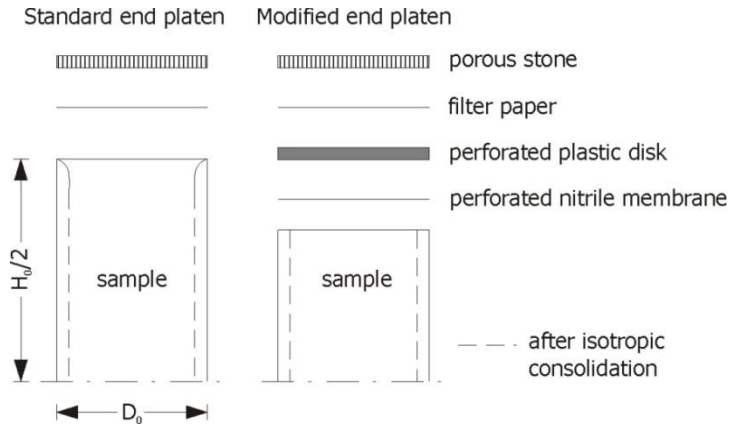

Fig. 2. Standard and modified end platens adopted in the present experimental investigation to reduce the end restraint

No silicone grease was applied between the perforated plastic disk and the nitrile membrane due to the difficulty in preventing contamination of the filter paper and the porous stone. Despite the present solution not assuring the same effectiveness as the one adopted by Rowe & Barden (1964), the lower friction between the nitrile membrane and the plastic disk, compared with the one at the interface between the filter paper and the porous stone, improves already the uniformity of stresses and strains. Not using enlarged platens was compensated by the significant lateral contraction experienced by the samples during isotropic consolidation. To assure perfect contact between the top cap and the load cell, a suction cap was used.

The samples were isotropically consolidated to a pre-consolidation mean effective stress p'_c of about 35 kPa (Table 1) and then sheared in undrained conditions at constant axial strain rate, $\dot{\varepsilon}_a$ = 0.02%/min. Four tests were conducted with standard rough end platens and height to diameter ratio increasing from H_0/D_0 = 1.5 to H_0/D_0 = 3. Sample 5 with H_0/D_0= 1.5, and sample 6 with H_0/D_0 = 2, were tested with modified end platens. The strain rate was chosen to theoretically assure pore pressure equalisation (Blight, 1963; Lade, 2016). The average axial strain rate experienced by sample 7, tested under drained K_0 stress control, is reported in Table 1.

Table 1. Index properties of the tested specimens and relevant information on the tests

Sample	Specific gravity Gs [-]	Initial void ratio e [-]	Organic content OC [-]	Stress path	Mean effective stress $p'_c = p'_0$ [kPa]	Initial height to diameter ratio H_0/D_0 [-]	End platens	Axial strain rate $\dot{\varepsilon}_a$ [% / min]
1	1.49	9.70	0.90	TxCU	35	1.5	Standard	0.02
2	1.49	9.80	0.90	TxCU	35	2.0	Standard	0.02
3	1.54	10.39	0.90	TxCU	34	2.5	Standard	0.02
4	1.49	9.64	0.90	TxCU	35	3.0	Standard	0.02
5	1.49	9.89	0.90	TxCU	34	1.5	Modified	0.02
6	1.47	9.59	0.90	TxCU	33	2.0	Modified	0.02
7	1.50	10.31	0.91	K_0	-	2.0	Standard	0.008

Stresses and strains measures

All the experimental data have been elaborated by adopting the common triaxial stress variables, namely the mean effective stress p', the deviatoric stress q and the corresponding strain variables, volumetric strain, ε_p, and deviatoric strain, ε_q. Natural strains were adopted due to the large displacements typically reached when testing peats (Ludwik, 1909; Hencky, 1928). The deviatoric strain has been computed from ε_p and ε_a derived from the volume change and the axial displacement measurements:

$$\varepsilon_p = \varepsilon_a + 2\varepsilon_r = \ln\left(\frac{V_0}{V}\right) \quad (1)$$

$$\varepsilon_q = \varepsilon_a - \frac{\varepsilon_p}{3} = \ln\left(\frac{H_0}{H}\right) - \frac{1}{3}\ln\left(\frac{V_0}{V}\right) \quad (2)$$

where V_0 and H_0 are the initial volume and height of the sample, while V and H are the current values.

EXPERIMENTAL RESULTS

Deviatoric stress-strain response

Shear stresses at the interface between the sample and the porous stone constrain the lateral expansion of the sample upon axial compression; hence, higher average axial stress and stiffness are expected. The impact on the calculated deviatoric response is reported in Fig. 3(a), where the deviatoric stress is normalised with the mean effective stress at the beginning of shear, p'_0. In Fig. 3(b) the calculated secant shear stiffness at 2% and 5% of deviatoric strain on the different samples are compared to each other.

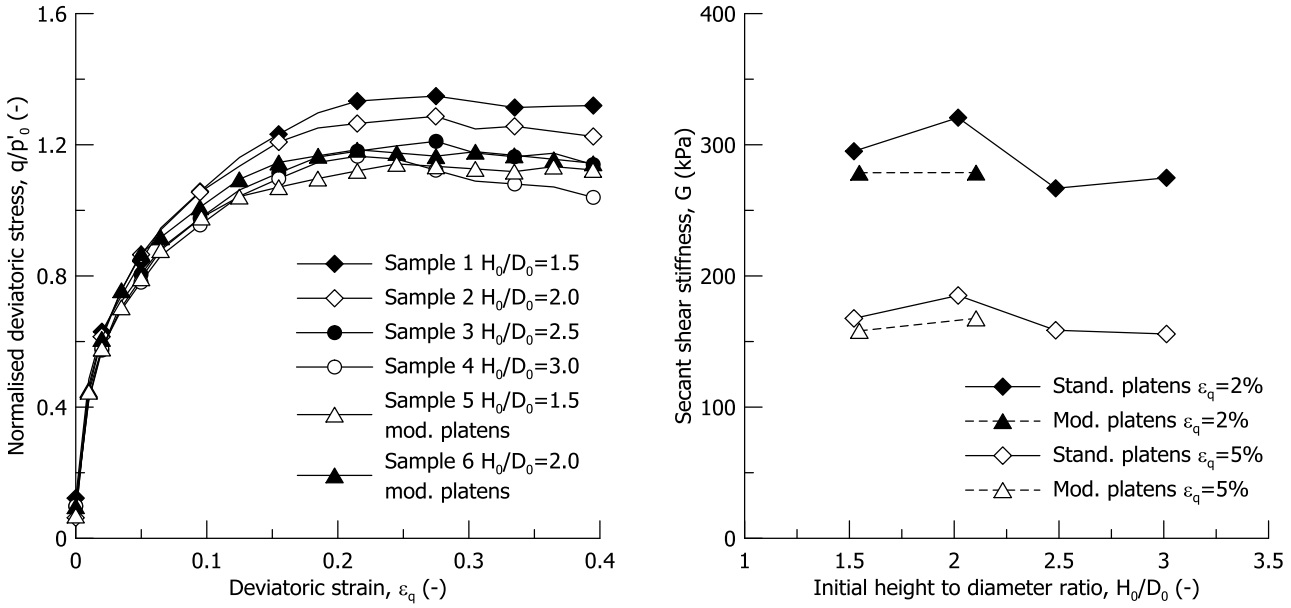

a) b)

Fig. 3. Deviatoric stress-strain response (a) and secant shear stiffness (b) upon undrained compression tests on samples with different height to diameter ratio tested with standard and modified end platens

The normalised deviatoric stress at failure decreases considerably with the height to diameter ratio towards the values calculated on sample 5 and sample 6, tested with modified end platens. The deviatoric stress levels off at about 25% of deviatoric strain, with the samples tested with modified end platens showing a more regular asymptotic response (Fig. 3(a)). The decrease in the deviatoric stress of sample 4 after $\varepsilon_q \cong 20\%$ is due to buckling occurring on the specimen. At small deviatoric strains, 2% - 5% (Fig. 3(b)), the modified end

platens slightly reduce the overall secant shear stiffness for the same height to diameter ratios compared to standard end platens, as in Duncan & Dunlop (1968) and Lade & Tsai (1985).

Excess pore pressure

The impact of end restraint on the excess pore pressure depends on the height to diameter ratio and on the friction between the sample and the end platens, and results in higher excess pore pressure at the top and bottom of the sample compared to its central portion (Rowe & Barden, 1964). Fig. 4 depicts the excess pore pressure measured at the bottom of the samples, Δu_w, using standard and modified end platens. The values are normalised with p'_0.

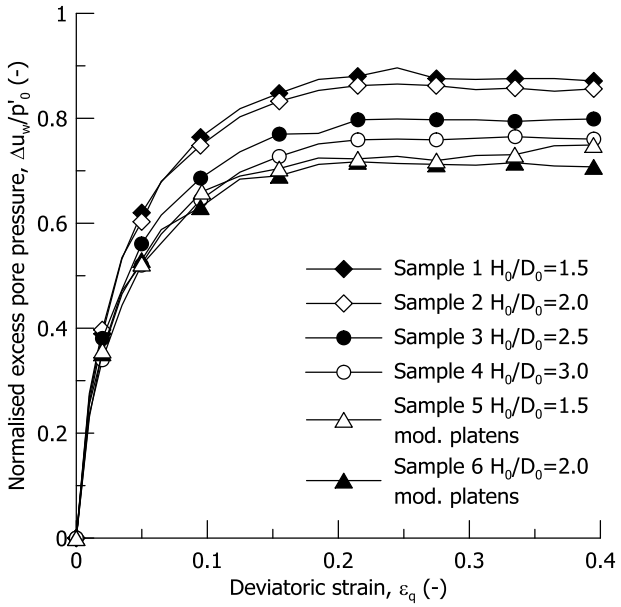

Fig. 4. Excess pore pressure measured at the bottom of the samples with different height to diameter ratio tested with standard and modified end platens

The excess pore pressure measured at the bottom decreases with the height to diameter ratio. For the shortest specimen tested with rough end platens, the excess pore pressure was 18% higher than when modified end platens were used. Compared to the commonly adopted ratio $H_0/D_0 = 2$, significant benefit was already found for $H_0/D_0 = 2.5$. However, the findings in Fig. 4 confirm that modified end platens are the most effective solution to avoid overestimation of the excess pore pressure, regardless the sample height to diameter ratio (sample 5 and sample 6). Benefits of low friction end platens on the pore pressure magnitude

are well documented in the literature for classical inorganic soils (Olson & Campbell, 1964; Barden & McDermott, 1965; Duncan & Dunlop, 1968 among others), but they had never been evaluated on peats.

Deformation mode and water content profile

Two aspects, among others, characterise the hydro-mechanical response of peats: a very high compressibility and relative low hydraulic conductivity, especially after the initial isotropic compression stage. The constraint due to rough end platens restrains the lateral deformation at the top and bottom of the sample, creating two so-called *dead zones*, and confines the unrestrained part, so-called *free failure zone*, to the central part of the sample (Fig. 5). The extension of the free-failure zone depends on both the shear strength and the compressibility of the soil (Rowe & Barden, 1964; Roscoe, 1970; Arthur et al., 1977; Drescher & Vardoulakis, 1982). Despite different hypothesis on the inclination of the dead zones, the combination of high compressibility and high friction angle of peats contributes to reducing the "free failure" zone upon axial compression. This is schematically depicted in Fig. 5. For the typical values of axial strain reached when testing peat in undrained compression tests, it is likely that the two dead zones merge and form connected dead wedges, which force lateral expansion of the external portion of the sample in the form of localised bulging, as displayed in Fig. 6(b). With the free failure zone reducing in size, the triaxial test loses representativeness as a soil "element" test.

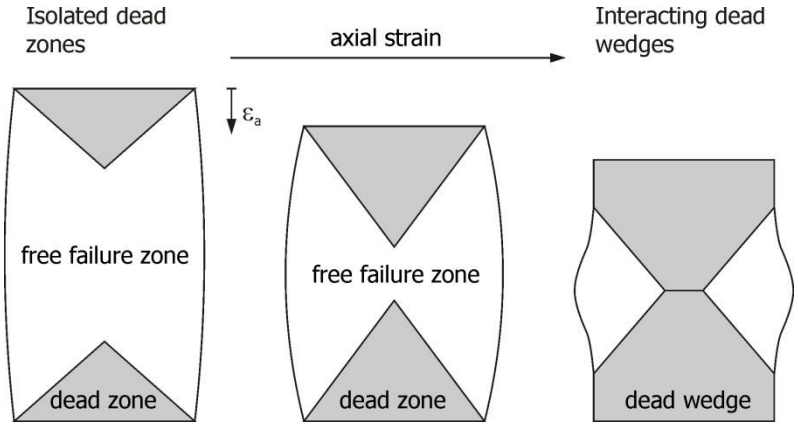

Fig. 5. Evolution of the free failure zone during axial compression on a peat sample tested with rough end platens

The kinematic constraint imposed by the end restraint results in a volume reduction of the soil within the dead zones, which is compensated by the expansion of the central portion of the sample. An internal water migration from the top and bottom of the sample towards the central portion occurs, despite the external undrained conditions. At the end of the test, each sample was rapidly dismounted and cut into three or more segments, depending on the failure mode, for water content determination. The similarity between the deformed shape of the sample and the measured water content profile can be appreciated in Fig. 6 for the case of sample 5 and sample 2, tested with modified and standard end platens respectively (w_{ave} is the average water content along the height of the sample measured at the end of each test). The deformed shape and the water content profile of sample 5 show significant uniformity thanks to the adoption of the modified end platens (Fig. 6(a)). On the contrary, the water content profile of sample 2 in Fig. 6(b) replicates the non-uniform deformation mode sketched in Fig. 5, with higher water content in the central portion.

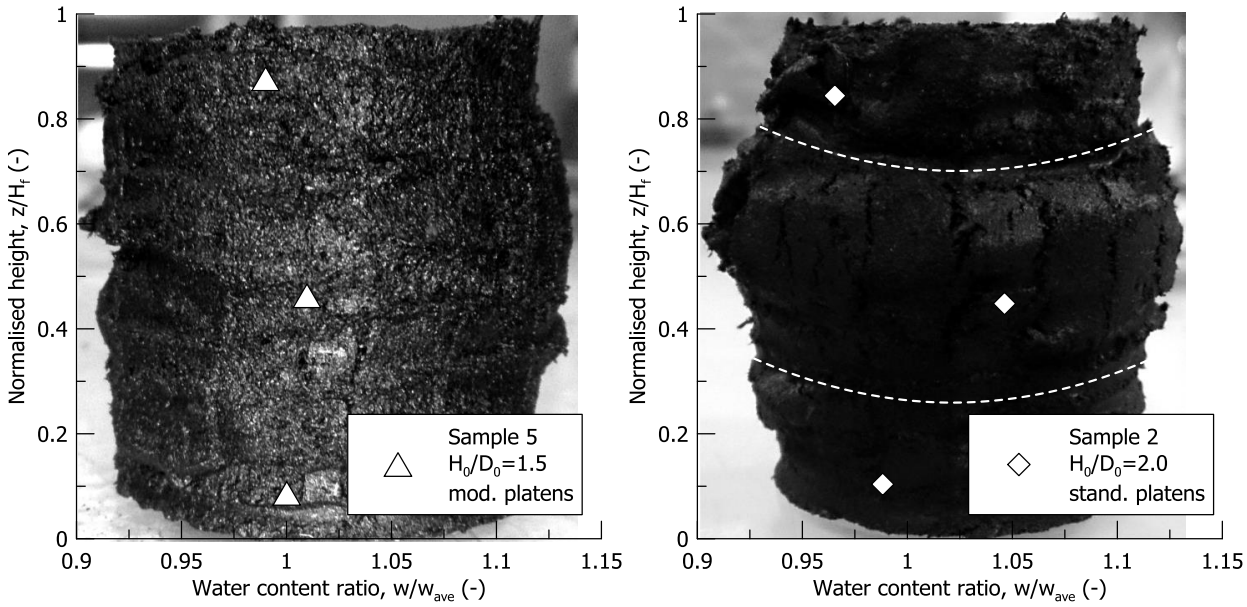

a) b)

Fig. 6. Analogy between the deformed shape and the water content profile in samples tested with (a) modified end platens and (b) standard end platens

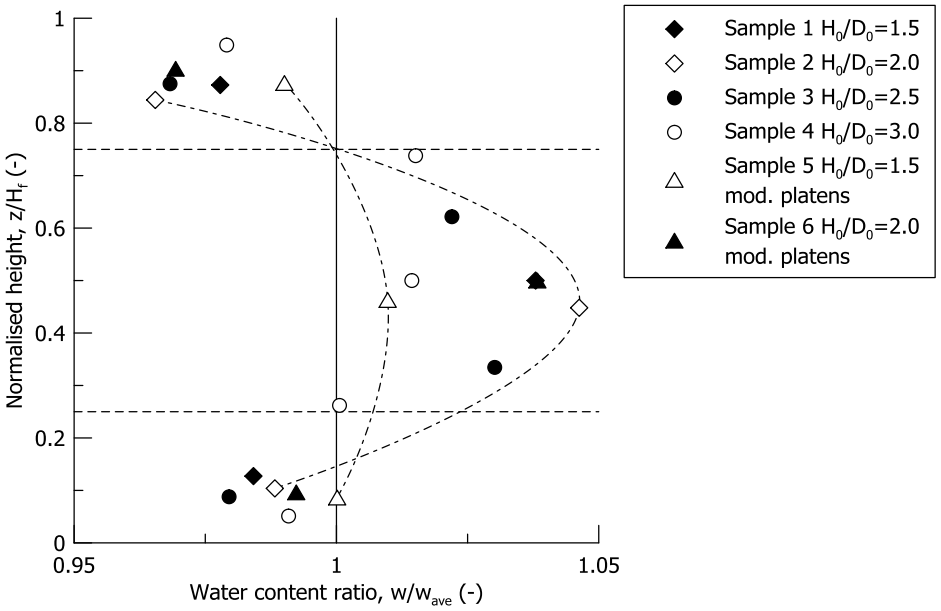

Fig. 7. Water content profiles at the end of undrained compression tests on samples with different height to diameter ratio tested with standard and modified end platens

The water content ratio w/w_{ave} profiles of all the samples at failure, shown in Fig. 7, clearly indicate that during the test water migrated from the top and the bottom of the sample towards the central portion. When standard end platens are used, the final water content in the central portion of the sample is 5% higher than the average one (with an experimental uncertainty of 6‰ on w/w_{ave}). The highest difference is found for the sample with $H_0/D_0 = 2$, while the tallest tested sample, $H_0/D_0 = 3$, shows a lower deviation, namely 2%. Only with modified end platens and short sample $H_0/D_0 = 1.5$ the measured water content is almost uniform within the sample.

Computed shear strength

The data show that end restraint affects the attained deviatoric stress, the water content distribution and the pore pressure measured at the base. The effects of end restraint on both the deviatoric stress and the excess pore pressure result in a dramatic influence on the ultimate friction angle derived from the maximum stress ratio attained during the test, which is reported in Fig. 8(a). The computed values of the friction angle for the different tests are reported in Fig. 8(b). Substantial reduction in the friction angle is observed for the samples tested with standard end platens by increasing the height to diameter ratio, passing from $\varphi' \cong 60°$ for

$H_0/D_0 = 1.5$ to $\varphi' \cong 45°$ for $H_0/D_0 = 3$. The samples tested with modified end platens reach failure for $\varphi' \cong 43°$, regardless their height to diameter ratio. The overestimation for standard $H_0/D_0 = 2$ sample tested with conventional end platens compared to the samples tested with modified end platens is about 12°, passing from $\varphi' \cong 43°$ to $\varphi' \cong 55°$.

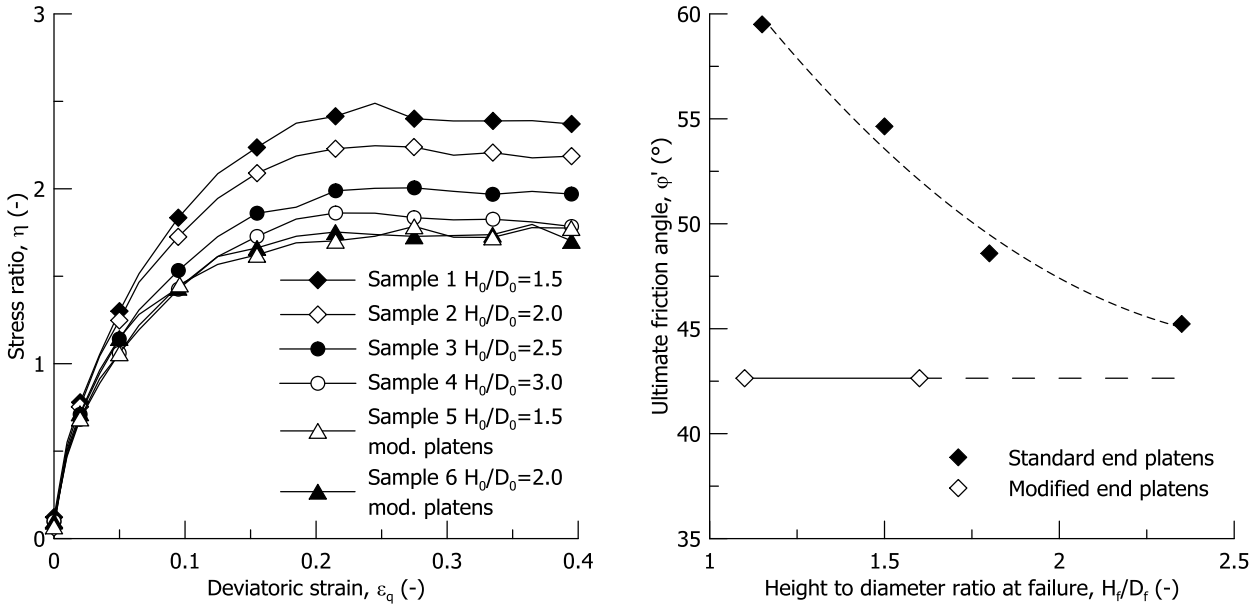

a) b)

Fig. 8. Stress ratio versus deviatoric strain (a) and ultimate friction angle (b) estimated for the samples with different height to diameter ratio tested with standard and modified end platens

To better investigate the physical reasons of these differences, in Fig. 9 the stress paths computed for the two samples having an initial $H_0/D_0 = 1.5$, tested with rough and modified end platens respectively, are compared to each other. The stress paths were computed by using the pore water pressure measurement at the base of the sample and estimating the deviatoric stress by using the cross sectional area of the volumetrically equivalent cylinder. The comparison clearly shows the twofold influence of end restraint on the computed stress path. Both overestimation of the current deviatoric stress and underestimation of the current mean effective stress contribute to the bias in the ultimate stress ratio, η_u, and justify the dramatic differences in the derived shear strength values. It is worth noting that these differences are affecting both the friction angle and the computed value of undrained shear strength.

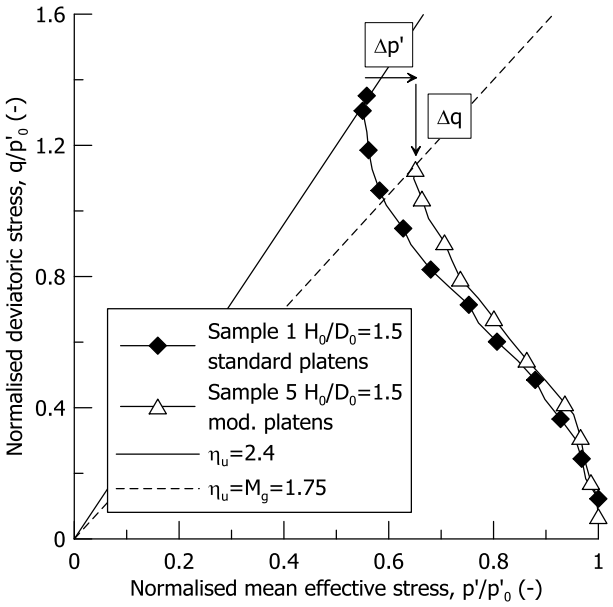

Fig. 9. Comparison between the normalised stress path followed on undrained compression by the samples with H_0/D_0 = 1.5 tested with standard and modified end platens

REDUCING THE CONSEQUENCES OF EXPERIMENTAL LIMITATIONS IN THE DETERMINATION OF SHEAR STRENGTH

The data presented allow quantifying the error introduced by end restraint on the determination of ultimate friction angle and undrained shear strength from standard undrained triaxial tests. Understanding the non-uniform response affecting both the apparent stress-strain relationship and the pore pressure measured at the base of the sample allows suggesting simple data elaboration procedures able to reduce the error in the determination of the shear strength parameters.

K_0 stress path

Previous works in the literature show that typical values of $K_0 \cong 0.30 - 0.35$ are obtained in strain controlled triaxial tests (Mitachi & Fujiwara, 1986; Edil & Wang, 2000; Mesri & Ajlouni, 2007; Hayashi et al., 2012). These values are much higher than those inferred from the simplified Jaky's equation, $K_0 \cong 1 - \sin\varphi'$ (Jaky, 1948) if the friction angle is estimated from uncorrected standard triaxial tests. This observation raised

doubts on the validity of Jaki's relationship for peats (Edil & Dhowian, 1981; Den Haan & Kruse, 2007; Leoni et al., 2010). The results presented in the previous section tend to suggest that the inconsistency may raise from inaccurate determination of the friction angle, rather then from lack in correlation between the two quantities. As a matter of fact, the K_0 stress path is the only one which is not affected at all by end restraint. This is due to the absence of any lateral strain, which avoids stress-strain non-uniformity and limits the fibres stretch contribution.

To clarify this aspect, an active K_0-compression test was performed on a sample with initial $H_0/D_0 = 2$ using rough end platens. The test was performed with an automated axial-radial stress ramp with volume change and axial displacement back measurements allowing for negligible radial strains. The data reported in Fig. 10 show that, starting form initial isotropic condition, the lateral stress ratio

$$K = \frac{3 - \eta}{3 + 2\eta} \tag{3}$$

where η is the current stress ratio, attains the final value $K_0 = 0.33$. The latter well fits the value inferred from Jaky's relationship, $K_0 = 0.32$, for the correct friction angle $\varphi' \cong 43°$ determined from samples with modified end platens, (sample 5 and sample 6, Fig. 8(b)).

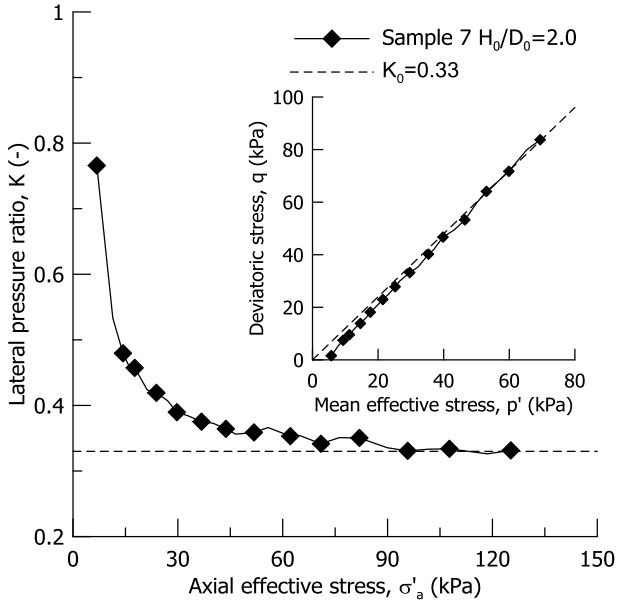

Fig. 10. Lateral stress ratio plotted against axial effective stress from the K_0-compression test

This result suggests that a K_0-compression test with active control could be useful in the determination of the shear strength from standard triaxial test data, as it gives a preliminary estimation of the ultimate friction angle, which is unbiased from stress and strain non-uniformities.

Correction for pore pressure non-uniformity

Better estimation of the ultimate friction angle does not solve all the issues related to the shear strength determination. The ultimate stress ratio is not an exhaustive information for undrained shear strength, which depends on the pore pressure developed while approaching failure. As a result, an error in the estimation of the pore pressure leads to a bias in the determination of a reliable value for undrained shear strength.

The experimental results show that end restraint produces higher excess pore pressure at the bottom of the sample compared to smooth end platens, and non-uniform profile of water content, which testifies the development of non-uniform pore pressure distribution. Local volume changes due to non-uniform deformation generate compression of the lower and upper parts of the sample and swelling of the central outer one, to comply with constant total volume constraint. With reference to Fig. 11, better insight into the mechanism can be attempted by representing the ideal stress-void ratio history of a soil element “a”, located inside the dead wedge, and an element “b”, located in the outer central portion of the sample.

As shown by Asaoka et al. (1994) and Asaoka et al. (1995), the soil elements “a” and “b” approach the failure line with volume reduction and volume increase, respectively. Divergence from the ideal undrained response progressively amplifies with the formation of the dead wedge and lateral bulging in the central portion of the sample. At the same time, the difference in pore pressure between the bottom and the mid height of the sample increases and becomes significant under small effective confining stresses on samples having low hydraulic conductivity (Oka et al., 2005; Kodaka et al., 2007). If the only available measurement of pore pressure is located at the bottom of the sample, a non-negligible error is introduced by end restraint in the estimation of the apparent effective stress path and in the undrained shear strength derived with reference to the measured quantities (Barden & McDermott, 1965; Blight, 1963; Sheng et al., 1997).

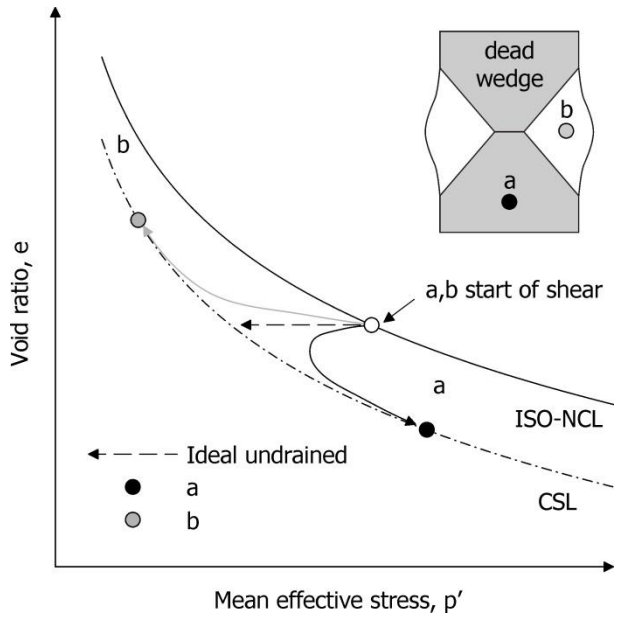

Fig. 11. Deviation of stress-void ratio history during axial compression in external undrained condition of two soil elements located in the dead wedge (a) and in the outer area of the middle part (b) due to end restraint

A simple procedure is suggested to estimate the pore pressure difference between the bottom (B) and the mid height of the sample (M), $\Delta u_{w,BM}$, and to correct the stress path. The water content profiles at the end of the test (Fig. 7) can be used to estimate the water mass change in the central portion of the sample ΔM_w over the test duration. A uniform distribution of water content is considered at the start of shear. With reference to Fig. 11, adopting the deviatoric strain as control variable, the change in mass of the centre of the sample over time, ΔM_w, can be represented by a function having null first order derivative at the start of shear and increasing rate while approaching failure. A simple second order polynomial, of the type $\Delta M_w = b\varepsilon_q{}^2$, satisfies these conditions, and can be adopted as a simple preliminary choice to model the water mass change at the centre of the sample over time. The result is displayed in Fig. 12 for three samples tested with rough end platens, normalised over the initial mass of water, M_{w0}.

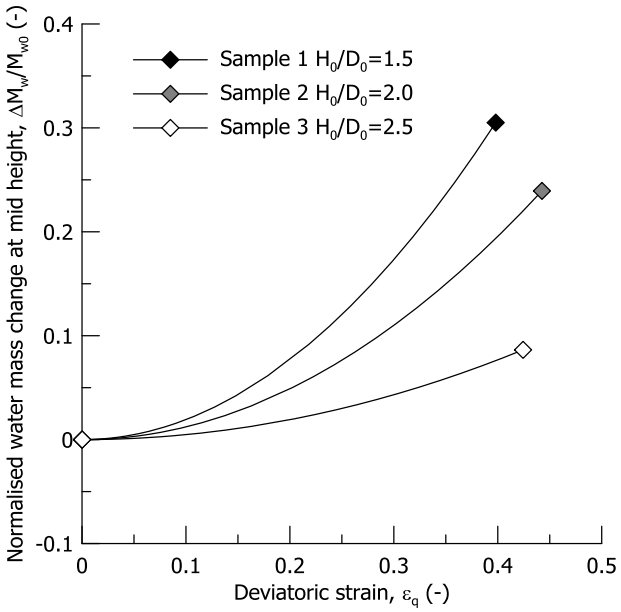

Fig. 12. Estimated evolution of the water mass change at the mid height of each sample with the deviatoric strain

If the internal flow rate from the top and bottom of the sample towards the centre is described by a simplified 1D flow field, the pore pressure difference between the bottom and the centre of the sample can be estimated to change over a time interval Δt as:

$$\Delta u_{w,BM} = -\frac{g}{4k_v}\frac{H}{A}\frac{\Delta M_w}{\Delta t} \qquad (4)$$

where g is the gravity acceleration, H is the current sample height, and A is the cross sectional area of the volumetrically equivalent cylinder (the derivation of equation (4) is reported in the Appendix). For the representative average void ratio of the samples at the start of shear, e = 7.0, the hydraulic conductivity was found to be $k_v \cong 1 \times 10^{-9}$ m/s (Zhao & Jommi, 2019). The estimated pore pressure at mid height of the sample over the shearing stage is compared with the measured one in Fig. 13, together with the excess pore pressure measured at the bottom of sample 5 tested with modified end platens. The comparison shows that the corrected pore pressure for the samples tested with rough platens well matches the one measured when smooth platens are used.

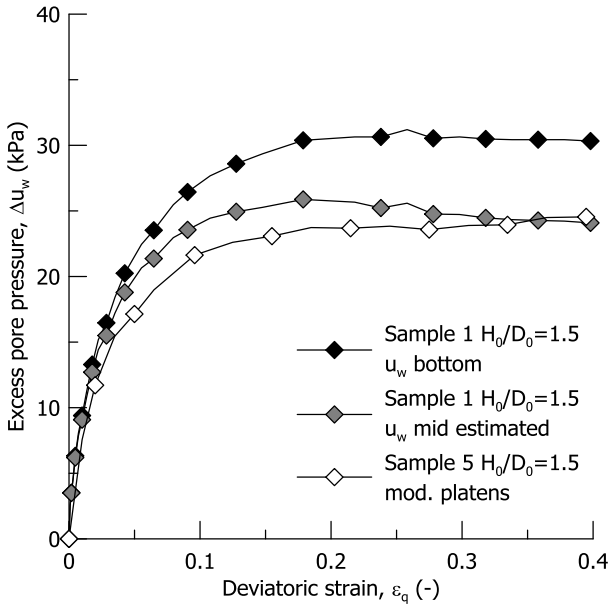

a)

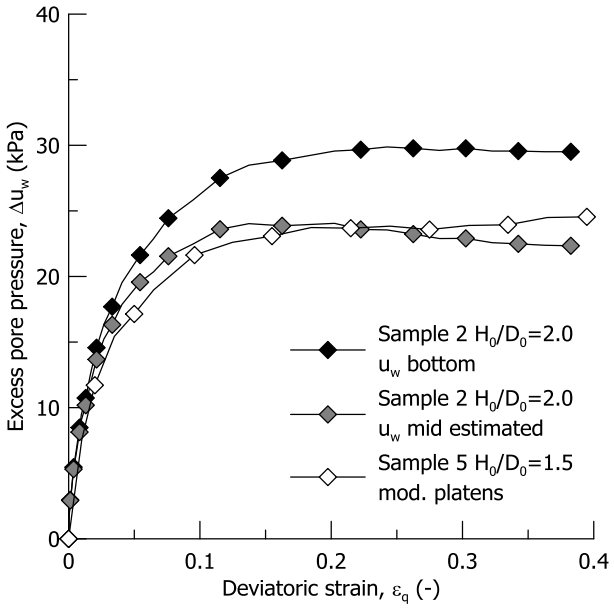

b)

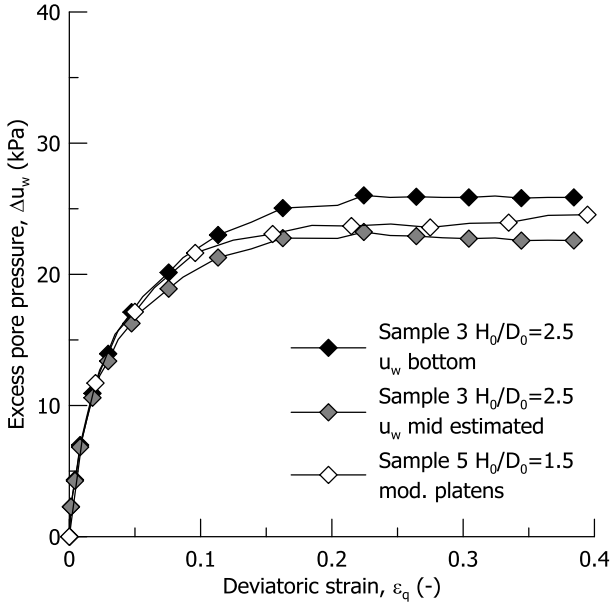

c)

Fig. 13. Excess pore pressure measured at the bottom and estimated at the mid height for (a) sample 1, (b) sample 2, and (c) sample 3 sheared with standard end platens and different height to diameter ratio

The benefits of correcting the stress path for the pore pressure difference between the base and the centre of sample are displayed in Fig. 14 in terms of normalised stress paths. The computed stress path with the corrected pore pressure much closer matches the stress path followed by sample 5 tested with modified end platens.

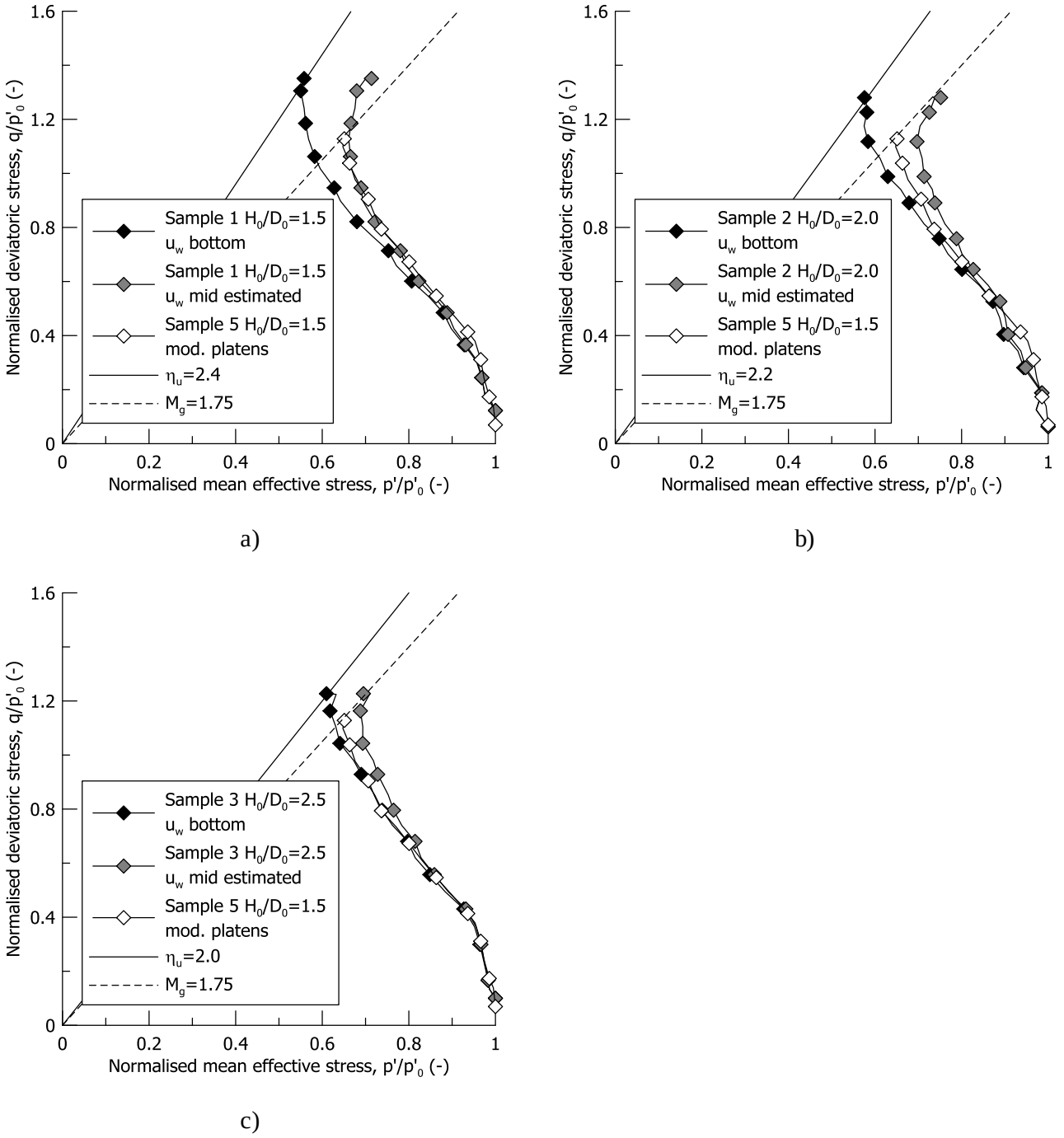

Fig. 14. Stress path calculated with the measured pore pressure at the bottom of the sample and with the estimated one at the mid height for (a) sample 1, (b) sample 2, and (c) sample 3

The correction reduces significantly the error introduced by the overestimation of the excess pore pressure at the bottom of the sample on the derivation of the stress path. Being aware of the overestimation of the deviatoric stress in Fig. 14, the information from the K_0-compression test presented in Fig. 10 can be used to

infer the correct ultimate friction angle. Therefore, by combining the results in Fig. 10 and Fig. 14 it is possible to obtain a reliable estimation of the undrained shear strength avoiding the bias due to end restraint effect on both the deviatoric stress and the excess pore pressure.

Complementary insight into the physical background of the proposed correction is given in Fig. 15, which plots the calculated pore pressure parameter, a, defined as (Wood, 1990):

$$a = -\frac{\Delta p'}{\Delta q} \tag{5}$$

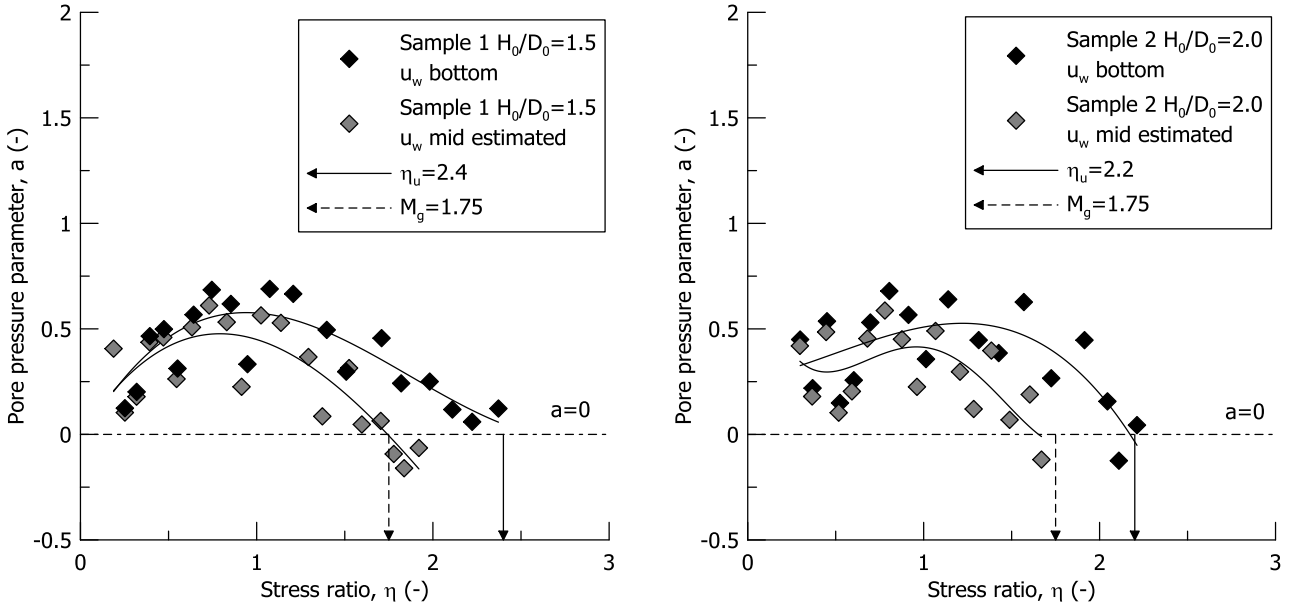

a) b)

Fig. 15. Pore pressure parameter corresponding to the stress path calculated with the measured pore pressure at the bottom of the sample and with the estimated pore pressure at the mid height for (a) sample 1 and (b) sample 2

The response of soil samples tested with rough end platens moves from a contractive regime, $a > 0$, towards an apparent dilatant regime, $a < 0$, passing through the condition $a = 0$ at the stress ratio which ideally identifies the critical stress ratio. Sample 1 and sample 2 attain $a = 0$ for a stress ratio $\eta_u = 2.4$ and $\eta_u = 2.2$, respectively. However, if the stress path is corrected for end restraint effect on the measured pore pressure,

the pore pressure parameter attains $a = 0$ for $\eta_u = 1.75$, which coincides with the ultimate stress ratio calculated from samples tested with modified end platens, and with the one inferred from the K_0 - compression test.

CONCLUSIONS

The dedicated experimental investigation brings to the forefront the role of end restraint in the interpretation of standard undrained triaxial tests on peat. The exceptional compressibility of this material, combined with high friction angles, increases the severity of stress and strain non-uniformities, introducing a relevant bias in the interpretation of the shear behaviour. The end restraint influence on the results was investigated on repeatable reconstituted samples of peat, to avoid the influence of heterogeneity of natural samples. Modified end platens were used on companion samples, to provide reliable reference data.

Standard rough end platens enhance end restraint effects, which leads to substantial overestimation of both the deviatoric stress and the pore pressure at failure. The error in the estimation of both quantities contributes to bias the determination of the friction angle and of the undrained shear strength from standard undrained triaxial compression test data. Tests on samples with standard height to diameter ratio initial $H_0/D_0 = 2$ using rough end platens gave an apparent friction angle $\varphi' = 55°$, which dramatically overestimates the "true" friction angle, $\varphi' = 43°$, obtained by reducing the platens friction.

Increasing the slenderness of the sample reduces the end restraint influence. However, a height to diameter ratio of at least 3 was necessary to obtain results close to the ones obtained with smooth end platens. The effectiveness of this practical choice is limited by the observation that slender samples easily undergo buckling, and by the geometrical limitations of standard equipment, which would require testing small diameter, hence less representative, samples.

Using end platens able to reduce the base friction clearly is the most effective protocol choice. When this is unfeasible, it is highly recommendable to correct the data interpretation for the error in the maximum deviatoric stress and for the difference between the pore pressure measured at the base and the pore pressure in the centre of the sample while approaching failure. A simple procedure was outlined to estimate the excess pore water pressure at the mid height of the sample when the only pore pressure measurement is taken at the bottom of the sample and rough end platens are used. The procedure requires an accurate measurement of the water content profile at the end of the test, and a reasonable estimate of the hydraulic conductivity of the peat for the representative void ratio. By calculating the stress path with the corrected pore pressure, most of the end restraint effect could be ruled out, with clear benefits on the estimated volumetric response and on the ultimate shear strength. Accompanying standard tests with an actively controlled K_0 stress path is recommended to clarify the "true" response of peats, as the kinematic constraint on null radial strains rules out end restraint effects. The K_0 value derived from the K_0-compression test performed with active control of null radial strains well matched the value obtained by means of Jaky's relationship from the undrained triaxial tests with smooth end platens.

The results reported in this work contribute to the reappraisal of triaxial tests in the study of shear strength of peats. For natural peats, it is expected that the higher hydraulic conductivity compared to the reconstituted samples will reduce the overestimation of the excess pore pressure at the bottom of the sample, for the same effective confining pressure. On the contrary, the presence of bigger fibres will amplify the end restraint effects on the deviatoric stress-strain response, hence, the overestimation of the deviatoric stress. Although the suggestions given in this work on how to correct for end restraint need to be verified on natural peat samples, highlighting the role of end restraint in the interpretation of the data will help in overcoming some of the current difficulties in the determination of shear strength of peats from standard triaxial tests.

ACKNOWLEDGEMENTS

The financial support of the Dutch Organisation for Scientific Research (NWO), under the project "Reliability-Based Geomechanical Assessment Tools for Dykes and Embankments in Delta Areas-13864 (Reliable Dykes)" is gratefully acknowledged. The Authors wish to thank Dr. Hongfen Zhao for her invaluable help and fruitful discussions.

APPENDIX

The different volumetric constraint at the top and bottom parts and at the centre of the sample promotes an internal water flow. The internal flow rate, q_w, , derived by a simplified 1D flow field, can be estimated as:

$$q_w = -\frac{k_v}{\gamma_w}\frac{\Delta u_{w,BM}}{H/2} \tag{6}$$

where k_v is the hydraulic conductivity in the vertical direction, γ_w is the unit weight of water and H is the current sample height. The corresponding mass of water flowing towards the central part of the sample in a time interval Δt can be estimated as:

$$\Delta M_w = 2\rho_w q_w A \Delta t \tag{7}$$

where ρ_w is the density of water and A is the cross sectional area of the volumetrically equivalent cylinder. Eq. (6) and eq. (7) give a mean to estimate the pore pressure difference between the bottom and the centre of the sample, $\Delta u_{w,BM}$, which reads:

$$\Delta u_{w,BM} = -\frac{g}{4k_v}\frac{H}{A}\frac{\Delta M_w}{\Delta t} \tag{8}$$

where g is the gravity acceleration, and , ΔM_w is the evolution of the water mass change in the central part of the sample during the time interval Δt. The hydraulic conductivity, k_v, of the tested peat was determined from an oedometer apparatus equipped with pore pressure transducers (Zhao & Jommi, 2019). Hydraulic conductivity in the order of $k_v \cong 1 \times 10^{-9}$ m/s was obtained for a void ratio of about 7.0, attained on average by the samples during the undrained shear. Given the total constant volume constraint and the small differences in void ratio caused by the flow, compared to the order of magnitude to the void ratio itself, a constant value can be assumed to analyse the process.

LIST OF SYMBOLS

H_0	initial sample height	(m)
D_0	initial sample diameter	(m)
V_0	initial sample volume	(m^3)
H	sample height	(m)
V	sample volume	(m^3)
H_f	sample height at failure	(m)
D_f	sample diameter at failure	(m)
Gs	specific gravity	
OC	organic content	
e	void ratio	
w	water content	
w_{ave}	average water content along the sample height at the end of the test	
M_w	mass of water	(kg)
ΔM_w	change of mass of water	(kg)
M_{w0}	mass of water at the mid height of the sample before shearing	(kg)
ρ_w	density of water	(kg/m^3)
γ_w	unit weight of water	(kN/m^3)
g	gravity acceleration	(m/s^2)
k_v	hydraulic conductivity in the vertical direction	(m/s)
q_w	internal flow rate	(m/s)
A	cross sectional area	(m^2)
ε_a	axial strain	
$\dot{\varepsilon}_a$	axial strain rate	(min^{-1})
ε_p	volumetric strain	
ε_q	deviatoric strain	

σ'_v	vertical effective stress	(kPa)
K	lateral stress ratio	
K_0	coefficient of earth pressure at rest	
G	secant shear stiffness	(kPa)
σ'_a	axial effective stress	(kPa)
p'	mean effective stress	(kPa)
p'_c	pre-consolidation mean effective stress	(kPa)
p'_0	mean effective stress at the beginning of shear	(kPa)
q	deviatoric stress	(kPa)
η	stress ratio	
η_u	ultimate stress ratio	
M_g	critical stress ratio	
φ'	friction angle	(°)
Δu_w	excess pore pressure	(kPa)
$\Delta u_{w,BM}$	difference of pore pressure between the bottom and the mid height of the sample	(kPa)
$\Delta p'$	change in the mean effective stress	(kPa)
Δq	change in the deviatoric stress	(kPa)
a	pore pressure parameter	
Δt	time interval	(s)
b	coefficient for the second order polynomial function	

LIST OF TABLES

LIST OF FIGURES

Fig. 10. Lateral stress ratio plotted against axial effective stress from the K_0-compression test

Fig. 11. Deviation of stress-void ratio history during axial compression in external undrained condition of two soil elements located in the dead wedge (a) and in the outer area of the middle part (b) due to end restraint

Fig. 12. Estimated evolution of the water mass change at the mid height of each sample with the deviatoric strain

Fig. 13. Excess pore pressure measured at the bottom and estimated at the mid height for (a) sample 1, (b) sample 2, and (c) sample 3 sheared with standard end platens and different height to diameter ratio

Fig. 14. Stress path calculated with the measured pore pressure at the bottom of the sample and with the estimated one at the mid height for (a) sample 1, (b) sample 2, and (c) sample 3

Fig. 15. Pore pressure parameter corresponding to the stress path calculated with the measured pore pressure at the bottom of the sample and with the estimated pore pressure at the mid height for (a) sample 1 and (b) sample 2

REFERENCES

Adams, J. I. (1961). Laboratory compression tests on peat. In *7th Muskeg Research Conference*. NCR, Ottawa, vol. 71, pp. 36–54.

Airey, D. W. (1984). Clays in circular simple shear apparatus. PhD thesis, University of Cambridge.

Arthur, J. R. F., Dunstan, T., Al-Ani, Q. A. J. L. & Assadi, A. (1977). Plastic deformation and failure in granular media. *Géotechnique* **27(1)**:53-74.

Asaoka, A., Nakano, M. & Noda, T. (1994). Soil-water coupled behaviour of saturated clay near/at critical state. *Soils and Foundations* **34(1)**:91-105.

Asaoka, A., Nakano, M. & Noda, T. (1995). Annealable behaviour of saturated clay: An experiment and simulation. *Soils and Foundations* **35(4)**:9-20.

Barden, L. & Mcdermott, J. W. (1965). Use of free ends in triaxial testing of clays. *Journal of the Soil Mechanics and Foundations Division* **91(6)**:1-23.

Bishop, A. W. & Green, G. E. (1965). The influence of end restraint on the compression strength of a cohesionless soil. *Géotechnique* **15(3)**:243-266.

Blight, G. E. (1963). The effect of nonuniform pore pressures on laboratory measurements of the shear strength of soils. In *Laboratory shear testing of soils*. ASTM International, vol. ASTM STP 361, pp. 173-184.

Boulanger, R. W., Arulnathan, R., Harder Jr, L. F., Torres, R. A. & Driller, M. W. (1998). Dynamic properties of Sherman Island peat. *Journal of Geotechnical and Geoenvironmental Engineering* **124(1)**:12-20.

Boylan, N. & Long, M. (2008). Development of a direct simple shear apparatus for peat soils. *Geotechnical Testing Journal* **32(2)**:126-138.

Budhu, M. (1984). Nonuniformities imposed by simple shear apparatus. *Canadian Geotechnical Journal* **21(1)**:125-137.

Cheng, X. H., Ngan-Tillard, D. J. M. & Den Haan, E. J. (2007). The causes of the high friction angle of Dutch organic soils. *Engineering Geology* **93(1)**:31-44.

Cola, S. & Cortellazzo, G. (2005). The shear strength behavior of two peaty soils. *Geotechnical and Geological Engineering* **23(6)**:679-695.

D1997-13 (2013). Standard test method for laboratory determination of the fiber content of peat samples by dry mass. *American Society of Testing and Materials*.

D2974-14 (2014). Standard test methods for moisture, ash, and organic matter of peat and other organic soils. *American Society of Testing and Materials*.

D5550-14 (2014). Standard test method for specific gravity of soil solids by gas pycnometer. *American Society of Testing and Materials*.

Den Haan, E. J. & Feddema, A. (2013). Deformation and strength of embankments on soft Dutch soil. *Proceedings of the Institution of Civil Engineers-Geotechnical engineering* **166(3)**:239-252.

Den Haan, E. J. & Grognet, M. (2014). A large direct simple shear device for the testing of peat at low stresses. *Géotechnique Letters* **4(4)**:283-288.

Den Haan, E. J. & Kruse, G. a. M. (2007). Characterisation and engineering properties of Dutch peats. In *Proceedings of the Second International Workshop of Characterisation and Engineering Properties of Natural Soils*. (Tan, Phoon, Hight, and Leroueil (eds)) Taylor & Francis Group, Singapore, vol. 29, pp. 2101-2133.

Drescher, A. & Vardoulakis, I. (1982). Geometric softening in triaxial tests on granular material. *Géotechnique* **32(4)**:291-303.

Duncan, J. M. & Dunlop, P. (1968). The Significance of Cap and Base Restraint in Strength Tests on Soils. *Journal of the Soil Mechanics and Foundations Division* **94(1)**:271-290.

Edil, T. B. & Dhowian, A. W. (1981). At-rest lateral pressure of peat soils. *Journal of Geotechnical and Geoenvironmental Engineering* **107(GT2)**:201-217.

Edil, T. B. & Wang, X. (2000). Shear strength and K0 of peats and organic soils. In *Geotechnics of high water content materials*. ASTM International, pp. 209-225.

Farrell, E. R. & Hebib, S. (1998). The determination of the geotechnical parameters of organic soils. In *Proc. of the Int. Symposium on Problematic Soils*. (Yanagisawa, Moroto, andMitachi (eds)) Balkema, Rotterdam, The Netherlands, vol. 98, pp. 33-36.

Farrell, E. R., Jonker, S. K., Knibbeler, A. G. M. & Brinkgreve, R. B. J. (1999). The use of direct simple shear test for the design of a motorway on peat. In *Geotechnical Engineering for Transportation Infrastructure: Theory and Practice, Planning and Design, Construction and Maintenance*: Proceedings of the Twelfth European Conference on Soil Mechanics and Geotechnical Engineering. (Barends, Lindenberg, Luger, Verruijt, andQuelerij, D. (eds)) CRC Press, Amsterdam, Netherlands, 7-10 June 1999, vol. 2, pp. 7-10.

Hayashi, H., Yamazoe, N., Mitachi, T., Tanaka, H. & Nishimoto, S. (2012). Coefficient of earth pressure at rest for normally and overconsolidated peat ground in Hokkaido area. *Soils and Foundations* **52(2)**:299-311.

Head, K. H. (2014). *Manual of soil laboratory testing – Vol. I: Soil classification and compaction tests*. Dunbeath, UK, Whitteles Publishing.

Head, K. H. & Epps, R. J. (2014). *Manual of soil laboratory testing – Vol. III: Effective stress tests*. Dunbeath, UK, Whitteles Publishing.

Hencky, H. (1928). Über die Form des Elastizitätsgesetzes bei ideal elastischen Stoffen. *Zeitschrift für technische Physik* **6**:215-220.

Hendry, M. T., Sharma, J. S., Martin, C. D. & Barbour, S. L. (2012). Effect of fibre content and structure on anisotropic elastic stiffness and shear strength of peat. *Canadian Geotechnical Journal* **49(4)**:403-415.

Jaky, J. (1948). State of stress at great depth. In *Proceedings of the Second International Conference of Soil Mechanics and Foundation Engineering* ,vol. 1, pp. 103-107.

Kanmuri, H., Kato, M., Suzuki, O. & Hirose, E. (1998). Shear strength of K0 consolidated undisturbed peat. In *Proc. of the Int. Symposium on Problematic Soils*. (Yanagisawa, Moroto, andMitachi (eds)) Balkema, Sendai, Japan, pp. 25-28.

Kodaka, T., Higo, Y., Kimoto, S. & Oka, F. (2007). Effects of sample shape on the strain localization of water-saturated clay. *International Journal for Numerical and Analytical Methods in Geomechanics* **31(3)**:483-521.

Komatsu, J., Oikawa, H., Ogino, T., Tsushima, M. & Igarashi, M. (2011). Ring Shear Test on Peat. In *The Twenty-first International Offshore and Polar Engineering Conference*. (Chung, Hong, Langen, andPrinsenberg (eds)), International Society of Offshore and Polar Engineers, Maui, Hawaii, USA, pp. 393-396.

Lade, P. V. (2016). *Triaxial testing of soils*. Chichester, West Sussex, UK, John Wiley & Sons.

Lade, P. V. & Tsai, J. (1985). Effects of localization in triaxial tests on clay. In *11th International Conference on Soil Mechanics and Foundation Engineering*, San Francisco, USA, vol. 2, pp. 549-552.

Landva, A. O. & La Rochelle, P. (1983). Compressibility and shear characteristics of Radforth peats. In *Testing of Peats and Organic Soils*. ASTM International, pp. 157-191.

Leoni, M., Karstunen, M. & Vermeer, P. (2010). Anisotropic creep model for soft soils (Discussion). *Géotechnique* **60(12)**:963-966.

Ludwik, P. (1909). *Elemente der Technologischen Mechanik*. Springer-Verlag.

Mesri, G. & Ajlouni, M. (2007). Engineering properties of fibrous peats. *Journal of Geotechnical and Geoenvironmental Engineering* **133(7)**:850-866.

Mitachi, T. & Fujiwara, Y. (1986). Consolidated undrained triaxial shear behavior of peat. *Bulletin of the Faculty of Engineering*, Hokkaido University **129**:1-14.

Muraro, S. & Jommi, C. (2019). Implication of end restraint in triaxial tests on the derivation of stress–dilatancy rule for soils having high compressibility. *Canadian Geotechnical Journal* **56(6)**: 840-851.

O'Kelly, B. C. (2017). Measurement, interpretation and recommended use of laboratory strength properties of fibrous peat. *Geotechnical Research* **4(3)**:136-171.

Ogino, T., Oikawa, H., Tsushima, M. & Mitachi, T. (2002). Strength Characteristics of Highly Organic Soil obtained by Direct Shear Tests. *Doboku Gakkai Ronbunshu* **715(60)**:277-285.

Oikawa, H. & Miyakawa, I. (1980). Undrained shear characteristics of peat. *Soils and Foundations* **20(3)**:91-100.

Oka, F., Kodaka, T., Kimoto, S., Ichinose, T. & Higo, Y. (2005). Strain localization of rectangular clay specimen under undrained triaxial compression conditions. In *Proceedings of the 16th International Conference on Soil Mechanics and Geotechnical Engineering*. Millpress Science Publishers, Lansdale, PA, vol. 16, pp. 841–844.

Olson, R. E. & Campbell, L. M. (1964). Discussion on importance of free ends in triaxial testing. *Journal of the Soil Mechanics and Foundations Division* **90(6)**:167-173.

Roscoe, K. H. (1970). The influence of strains in soil mechanics. *Géotechnique* **20(2)**:129-170.

Rowe, P. W. & Barden, L. (1964). Importance of free ends in triaxial testing. *Journal of Soil Mechanics & Foundations Division* **90(1)**:1-27.

Rowe, R. K., Maclean, M. D. & Soderman, K. L. (1984). Analysis of a geotextile-reinforced embankment constructed on peat. *Canadian Geotechnical Journal* **21(3)**:563-576.

Sheng, D., Westerberg, B., Mattsson, H. & Axelsson, K. (1997). Effects of end restraint and strain rate in triaxial tests. *Computers and Geotechnics* **21(3)**:163-182.

Shockley, W. G. & Ahlvin, R. G. (1960). Nonuniform conditions in triaxial test specimens. In *Research Conference on Shear Strength of Cohesive Soils*. ASCE, University of Colorado, Boulder, Colorado, pp. 341-357.

Stark, T. D. & Vettel, J. J. (1992). Bromhead ring shear test procedure. *Geotechnical Testing Journal* **15(1)**:24-32.

Tashiro, M., Nguyen, S. H., Inagaki, M., Yamada, S. & Noda, T. (2015). Simulation of large-scale deformation of ultra-soft peaty ground under test embankment loading and investigation of effective countermeasures against residual settlement and failure. *Soils and Foundations* **55(2)**:343-358.

Wood, D. M., Drescher, A. & Budhu, M. (1979). On the determination of stress state in the simple shear apparatus. *Geotechnical Testing Journal* **2(4)**:211-221.

Yamaguchi, H., Ohira, Y., Kogure, K. & Mori, S. (1985). Undrained shear characteristics of normally consolidated peat under triaxial compression and extension conditions. *Soils and Foundations* **25(3)**:1-18.

Yamaguchi, H., Yamauchi, K. & Kawano, K. (1987). Simple shear properties of peat. In *Proc. Int. Symp. on Geotechnical Engineering of Soft Soils*. Sociedad Mexicana de Mecánica de Suelos, Coyoacán, Mexico, vol. 1, pp. 163-170.

Zhang, L. & O'Kelly, B. C. (2014). The principle of effective stress and triaxial compression testing of peat. *Proceedings of the Institution of Civil Engineers-Geotechnical Engineering* **167(1)**:40-50.

Zhao, H.F. & Jommi, C. (2019). Consequences of drying on the fabric and the compression behaviour of a Dutch fibrous peat. Submitted to *Canadian Geotechnical Journal*.

Zwanenburg, C., Den Haan, E. J., Kruse, G. A. M. & Koelewijn, A. R. (2012). Failure of a trial embankment on peat in Booneschans, the Netherlands. *Géotechnique* **62(6)**:479-490.